

INTERFERENCE COEFFICIENTS FOR OVERLAPPING OXYGEN LINES IN AIR

P. W. ROSENKRANZ

Research Laboratory of Electronics, Massachusetts Institute of Technology, Cambridge,
MA 02139, U.S.A.

(Received 3 July 1987)

Abstract—Interference coefficients describe the non-Lorentzian effect that arises as pressure broadening causes lines to overlap. These coefficients, one for each line, are at moderate pressures related linearly to absorption and dispersion. They are determined here for the 5-mm wavelength oxygen lines broadened by air. The method includes four *a priori* constraints on off-diagonal elements of the relaxation matrix, which produce the interference effect: (1) detailed balance; (2) intra-branch submatrices are assumed to be identical; (3) coupling between the + and – branches is ignored; (4) coupling between the (positive-frequency) resonances and the nonresonant and negative-resonant branches is represented by a small bias term in the interference coefficients. The linear equations relating measured dispersion to the interference coefficients are solved by the Twomey–Tikhonov method, which minimizes a cost function, subject to the condition of constant measurement–error variance. The cost function is chosen to minimize the variation of elements along diagonals of the intra-branch relaxation submatrix. Implications for atmospheric radiative transfer are briefly discussed.

1. INTRODUCTION

When pressure broadening causes two or more lines to overlap, deviations from a sum of Lorentzian line shapes are often observed. This effect is termed interference, mixing, coupling, blending, or merging of lines. Some of the molecules for which it has been observed to be significant are O₂,^{1–3} CO₂,^{4,5} CO,^{5,6} N₂,⁶ and N₂O.⁵ Theoretical expressions for the shape of bands of overlapping lines were first developed by Baranger⁷ and Kolb and Griem,⁸ and rederived in a more general context by Fano.⁹ The influence of collision dynamics on the spectrum is expressed through a relaxation matrix. This matrix can, at least in the limit of instantaneous collisions (impact approximation), be calculated from first principles and a given intermolecular potential (see Refs. 10–13 for O₂).

These calculations are highly computation-intensive; therefore, models for the relaxation matrix, such as the strong-collision,⁴ exponential-gap⁴ and tridiagonal¹⁴ model have been found useful to interpret measurements. Models certainly have a place in interpretation of spectra; however, when computations based on models with restrictive assumptions show small disagreements with radiometric measurements (e.g., Ref. 15), it may be unclear where to seek resolution of the discrepancy.

It should be fruitful to consider the experimentalist's task of measuring parameters from the standpoint of estimation theory. If one considers l lines, a relaxation matrix has dimensions $2l \times 2l$. At moderate pressure, its influence on the spectrum can be reduced to $2l$ parameters: l linewidths and l interference parameters.¹⁴ Moderate pressures may be defined as roughly those for which the dimensionless interference parameters are smaller than unity. We describe a method of inverting the linear equations relating measured dispersion (or absorption) to the interference parameters, at moderate pressures. This method is robust in the presence of measurement errors. The spin-rotation band of O₂ will be the subject of the discussion.

2. MILLIMETER-WAVE ABSORPTION AND REFRACTION IN OXYGEN

Oxygen is a paramagnetic substance, with a molecular dipole moment of two Bohr magnetons due to the presence of two unpaired electron spins.¹⁶ In the electronic ground state, the spin vector

combines with rotational angular momentum (Hund's coupling case b) to form a triplet of energy levels with total angular momentum $J = N - 1$, N , and $N + 1$, for each value of rotational quantum number N . Symmetry of the molecular wavefunction with respect to the two identical nuclei restricts N to odd values, and states up to $N \sim 33$ are significantly populated at atmospheric temperatures. With one exception, the transition frequencies for $J = N$ to $N - 1$, denoted ν_{N-} , and $J = N$ to $N + 1$, denoted ν_{N+} , lie between 50 and 70 GHz. The magnetic dipole moment also has nonzero diagonal matrix elements which, as a result of reorientation by collisions, contribute nonresonant absorption throughout the microwave spectrum.¹⁶

At pressures approaching 1 bar, the lines are broadened by collisions to form a continuous band. Within the impact approximation, the power absorption coefficient can be written as^{7,8,17}

$$\alpha(\nu) = \frac{8\pi^2 n_a \nu^2}{3ckTQ} \sum_{i=0}^l a_i \left[\frac{\gamma_i + Y_i(\nu - \nu_i)}{(\nu - \nu_i)^2 + \gamma_i^2} + \frac{\gamma_i - Y_i(\nu + \nu_i)}{(\nu + \nu_i)^2 + \gamma_i^2} \right], \quad (1)$$

where ν is the observation frequency, n_a is the number of absorbing molecules per unit volume, T is temperature, ν_i is a line frequency, γ_i is a line half-width, Y_i is a line interference parameter, and a_i is proportional to a line strength. The partition function is $Q = \sum_N 3(2N + 1) \exp(-E_N/kT)$, where E_N is the energy of the level $J = N$. Corresponding to Eq. (1) there is an associated equation for the refractive index.¹⁷ The dispersive part is given by

$$N(\nu) - N(0) = \frac{2\pi n_a \nu}{3kTQ} \sum_{i=0}^l a_i \left[\frac{\nu_i - \nu + Y_i \gamma_i}{(\nu - \nu_i)^2 + \gamma_i^2} - \frac{\nu_i + \nu + Y_i \gamma_i}{(\nu + \nu_i)^2 + \gamma_i^2} \right]. \quad (2)$$

In Eqs. (1) and (2), the approximation $\nu_i \ll kT/h$ has been employed, and c , k and h have their standard meanings.

To first order, ν_i and a_i are independent of pressure: $\nu_i = \nu_{N+}$ or ν_{N-} and $a_i = \mu_i^2 \exp(-E_N/kT)$, in which μ_i is the reduced dipole moment matrix element; i.e., $\mu_{N-}^2 = 4\mu_B^2(N + 1)(2N - 1)/N$ and $\mu_{N+}^2 = 4\mu_B^2 N(2N + 3)/(N + 1)$, where μ_B is the Bohr magneton. The nonresonant component of absorption is included in the summations as $i = 0$, with line frequency and interference parameter set to zero, and with $a_0 = 1.40 \mu_B^2 Q$. The absence of first-order pressure terms in ν_i and a_i is a consequence of the pure-imaginary character of the relaxation matrix for this band of O_2 .^{13,18,19}

To lowest order, γ_i and Y_i are proportional to pressure; they can be related to the elements of a relaxation matrix by^{14,19}

$$\gamma_i = \mathbb{M}_{ii}'', \quad (3a)$$

$$Y_i = \frac{2}{\mu_i} \sum_{\substack{j=-l \\ j \neq i}}^l \frac{\mu_j \mathbb{M}_{ji}''}{\nu_i - \nu_j}. \quad (3b)$$

\mathbb{M}'' is the negative imaginary part of the relaxation matrix defined by Fano.⁹ The summation in Eq. (3b) extends over negative resonant frequencies $\nu_{-j} = -\nu_j$ as well as the positive ν_j and $\nu_0 = 0$. The ν_{-j} are associated with the second term inside the square brackets in Eqs. (1) and (2). From the fundamental requirement that $\alpha(\nu)$ and $N(\nu)$ be even functions of ν , it follows that $\gamma_{-i} = \gamma_i$ and $Y_{-i} = -Y_i$; these equalities have already been taken into account in writing Eqs. (1) and (2). The first-order equations provide an accurate approximation to the band shape, even at pressures near 1 bar where the line overlap is appreciable, because of partial cancellation of higher order terms.¹⁹

3. INVERSION OF REFRACTION MEASUREMENTS

Determination of the relaxation matrix (or of the γ s and Y s) is the central problem in describing bands of overlapped lines. When pressure is sufficiently low that line overlap is negligible, the line shape near resonance is nearly Lorentzian, and interpretation of measurements to obtain linewidth parameters is unambiguous.²⁰ The effect of the interference parameters becomes detectable only as the pressure is increased. Dispersion can be measured more precisely than absorption, so the discussion here will focus on interpretation of the dispersion measurements at pressures of 400–800 torr (533–1067 mbar) described by Liebe et al.;¹ however, similar comments would apply to absorption. Liebe's spectrometer²⁰ measures the quantity $\Delta N = N(\nu) - N(\nu/2)$. Table 1 lists the

Table 1. Measured¹ and calculated dispersion in dry air at 300 K. Estimated measurement uncertainty is ± 10 ppb (1 ppb = 10^{-9}). Calculations use the coefficients in Table 2.

Vacuum tuning frequency (GHz)	Nearby line center	Dispersion (ppb) at							
		400 torr		500 torr		600 torr		800 torr	
		mea- sured	calcu- lated	mea- sured	calcu- lated	mea- sured	calcu- lated	mea- sured	calcu- lated
53.5957	25-	300	301			430	439		
54.1300	23-	350	338			500	490		
55.2214	19-	400	406			580	574		
55.7838	17-	420	420	510	506	600	587	720	734
56.3634	15-, 1+	410	397			590	563		
56.9682	13-	380	347			450	499	650	628
58.4466	3+, 9-	200	172			280	249		
59.1642	7-	80	73			120	105		
59.5910	5+	30	24			30	26		
60.3040	5-, 7+	-75	-89			-90	-140		
60.4330	7+, 5-	-155	-127			-170	-177		
61.1490	9+	-275	-257			-383	-369		
61.7980	11+	-335	-347			-510	-530		
62.4090	13+, 3-	-480	-482			-685	-695		
62.4840	3-, 13+	-510	-501	-650	-611	-720	-714		
62.9960	15+	-590	-586	-680	-701	-790	-810		
63.5670	17+	-610	-596	-690	-723	-841	-842	-1080	-1058

measured values of ΔN . For air, the frequency of measurement ν is related to the vacuum tuning frequency ν_R by¹

$$\nu = \nu_R(1 - 1.0356 \times 10^{-4} P/T), \quad (4)$$

with P given in torr and T in Kelvin. The frequencies ν_R were chosen to lie on or near line centers.

3.1. Weighting factors

Let the measurements be indexed by a subscript k and let ΔN_k^0 be the value of ΔN_k computed by setting the Y s equal to zero. Having measurements at several values of pressure P , it is more convenient to work with the coefficients $y_i = Y_i/P$. Then Eq. (2) implies that

$$\Delta N_k - \Delta N_k^0 = \sum_{i=1}^I W_{ki} y_i + \epsilon_k, \quad (5)$$

where, because the interference coefficients have virtually no influence on refraction near 30 GHz,

$$W_{ki} = \frac{2\pi n_a P \nu a_i}{3kTQ} \left[\frac{\gamma_i}{(\nu - \nu_i)^2 + \gamma_i^2} - \frac{\gamma_i}{(\nu + \nu_i)^2 + \gamma_i^2} \right], \quad (6)$$

and ϵ_k is the combination of error in measured ΔN_k and the error resulting from use of experimentally determined linewidths (from resolved lines) to compute ΔN_k^0 . The fundamental difficulty in solving the system of Eq. (5) for the y s is that it is ill-conditioned. At low pressure, the interference effect, $\Delta N - \Delta N^0$, is small, and increasing pressure broadens the lines so that each measurement

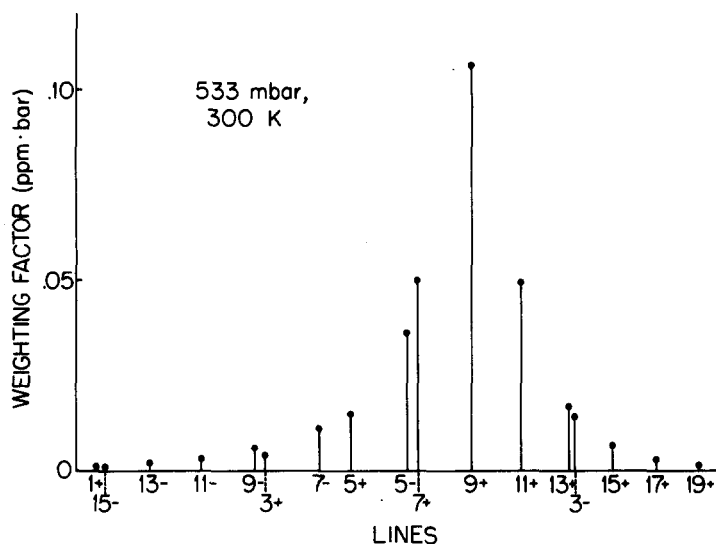


Fig. 1. Weighting factors for the contribution of interference coefficients to dispersion measured at the 9+ line center. The lines are plotted by frequency.

is a superposition of effects from several interference parameters. Figure 1 is a plot of the weights W_{ki} for a measurement at the 9+ line, illustrating the significant amount of broadening even at 400 torr. The overlap of the + and - branches of the oxygen spectrum only increases the difficulty of the problem.

In general, there are two approaches to solving an ill-conditioned system in the presence of measurement errors. One is to employ a model having a small number of adjustable parameters; this is the method used by Liebe et al.¹⁻³ The other approach is to stabilize the inversion operation by incorporation of *a priori* information or constraints. Many techniques for accomplishing this stabilization have been developed for inverse problems occurring in remote sensing.²¹ Preferably, the constraints will be based on physical considerations. In the case of pressure broadening, the appropriate object on which to impose constraints is the relaxation matrix.

3.2. Constraints on M''

The first constraint is related to the principle of detailed balance:

$$M''_{ji} = M''_{ij} \exp[(E_i - E_j)/kT], \quad (7)$$

where E_i is the initial energy level of line i . This constraint has a firm theoretical basis.²²

Next, it will be assumed that the submatrix of M'' coupling lines within the + branch of the spectrum is identical to the submatrix that couples lines within the - branch. This constraint is exact in Gordon's¹⁸ semi-classical theory of the oxygen band, and is supported to a good approximation by the fully quantum-mechanical calculation of Lam.¹² Experimental support for it can be inferred from the closeness of the widths of lines $N+$ and $N-$.¹⁻³ The upper-right, off-diagonal triangle of this intra-branch submatrix will be represented by $R(N', N)$, with $N' < N$, where N' and N are the quantum numbers associated with the two lines coupled by an element of R .

Elements of M'' that couple lines in the + branch to lines in the - branch will be assumed to be zero. In Lam's¹² calculations, these elements are much smaller than many of the elements $R(N', N)$. This result has been explained by Smith¹⁹ on the basis of a tendency for the electron spin vector to be unchanged by molecular collisions.

Equation (3b) expresses the interference parameter for each line as a summation over all other line frequencies to which it is coupled. One might think that it would be safe to neglect the terms that couple positive ν_i to negative or zero ν_j , because of the large frequency differences in the denominator. In i.r. spectra these terms would no doubt be truly negligible. In the oxygen microwave band they make only a small contribution to the Y s, but in the same direction for each

line. It will be seen below that their cumulative effect is detectable in atmospheric measurements made on the far wings of the band. The contribution of these terms is too small to be reliably determined from the available dispersion measurements, but it can be estimated from Gordon's¹⁸ theory. He pointed out that at large frequency displacements, a band can be replaced by a common resonance. For oxygen, M'' reduces to a 3×3 matrix with diagonal elements equal to γ_0 , the nonresonant broadening parameter, and off-diagonal elements equal to $-\gamma_0/2$. To this approximation, the contribution to y_i of the terms that couple line i to the zero- and negative-frequency transitions is given by¹⁴

$$b_i = -\gamma_0/Pv_i - \gamma_0/P(v_i + 60 \text{ GHz}). \quad (8)$$

Because the nonresonant transitions have an exactly common frequency of zero, collisions contribute to γ_0 only through reorientation of the angular momentum vector; it is therefore smaller than the γ_i .¹⁸ Measurements indicate that a reasonable value for γ_0/P is 0.48 GHz/bar.¹⁴ Thus, $b_i \sim -0.012 \text{ bar}^{-1}$.

By arranging the elements of $r(N', N) = R(N', N)/P$ as a vector \mathbf{r} and including \mathbf{b} as a bias vector, the indicated constraints allow us to substitute for Eq. (3b) the following relation:

$$\mathbf{y} = \mathbb{K} \mathbf{r} + \mathbf{b}. \quad (9)$$

An element of the matrix \mathbb{K} in row i and column corresponding to (N', N) is

$$K(i, N', N) = \delta(N_i, N) \frac{2\mu_{N'}}{\mu_i(v_i - v_{N'})} + \delta(N_i, N') \frac{2\mu_N}{\mu_i(v_i - v_N)} \exp(E_N - E_{N'})/kT, \quad (10)$$

where N_i is the quantum number associated with line i , μ_N and v_N are the dipole element and frequency of the line associated with quantum number N and in the same branch as line i , and $\delta(N_i, N)$ is the Kronecker delta. Because of the restriction $N' < N$, Eq. (7) has been used in Eqn. (10) to provide the contribution from the opposite half of the relaxation matrix.

3.3. Solution by the Twomey-Tikhonov method

Defining $g_k = \Delta N_k - \Delta N_k^b$, where ΔN_k^b is the dispersion computed by setting $y_i = b_i$, we combine Eqs. (5) and (9) into

$$\mathbf{g} = \mathbb{A} \mathbf{r} + \boldsymbol{\epsilon} \quad (11)$$

with $\mathbb{A} = \mathbb{W} \mathbb{K}$. The system (11) is still ill-conditioned and also underdetermined, since \mathbf{r} contains well over a hundred elements. Therefore its solution requires a stabilized inversion method.

The method devised by Twomey²³ and Tikhonov²⁴ can be adapted to the present problem. Recognizing that any vector \mathbf{r} is an acceptable solution if it satisfies (11) with $\boldsymbol{\epsilon}^T \boldsymbol{\epsilon} \leq ne^2$, where e^2 is the error variance of n measurements, Twomey proposes to select, from the set of acceptable vectors, the one that minimizes a cost function $q = \mathbf{r}^T \mathbb{H} \mathbf{r}$, where \mathbb{H} is a matrix to be specified. Assuming \mathbb{H} to be positive definite, the absolute minimum of q is attained with $\mathbf{r} = 0$. If $\mathbf{r} = 0$ is not an acceptable solution, then because of the quadratic form of q , its minimum value within the set of acceptable \mathbf{r} s will be attained on the boundary of that set; i.e., when $\boldsymbol{\epsilon}^T \boldsymbol{\epsilon} = ne^2$. Twomey finds the solution as the vector \mathbf{r} with respect to which the quadratic expression

$$(\mathbb{A} \mathbf{r} - \mathbf{g})^T (\mathbb{A} \mathbf{r} - \mathbf{g}) + \beta \mathbf{r}^T \mathbb{H} \mathbf{r}$$

is stationary, with β a Lagrange multiplier. The result is²³

$$\mathbf{r} = (\mathbb{A}^T \mathbb{A} + \beta \mathbb{H})^{-1} \mathbb{A}^T \mathbf{g}; \quad (12)$$

or equivalently,

$$\mathbf{r} = \mathbb{H}^{-1} \mathbb{A}^T (\mathbb{A} \mathbb{H}^{-1} \mathbb{A}^T + \beta \mathbb{I})^{-1} \mathbf{g}, \quad (13)$$

where \mathbb{I} is the identity matrix. The value of β will be determined to satisfy the error variance.

The corresponding solution for the interference coefficients is obtained from Eq. (9):

$$\mathbf{y} = \mathbb{S} \mathbb{W}^T (\mathbb{W} \mathbb{S} \mathbb{W}^T + \beta \mathbb{I})^{-1} \mathbf{g} + \mathbf{b}, \quad (14)$$

in which $\mathbb{S} = \mathbb{K} \mathbb{H}^{-1} \mathbb{K}^T$ plays the role of an inverse cost matrix for \mathbf{y} .

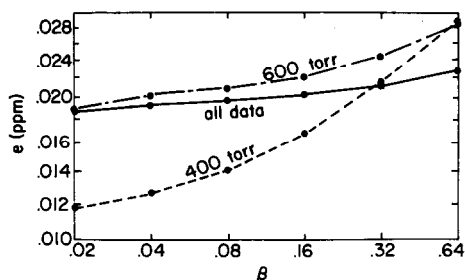


Fig. 2. R.m.s. residuals e , as a function of the Lagrange multiplier β , for the entire set of measurements in Table 1 and for two subsets (1 ppm = 10^{-6}).

3.6. Results and comparison with other work

Application of Eq. (14) with $\beta = 0.16$ to all of the measurements in Table 1 yields the y_s listed in Table 2. Computed values of dispersion are given in Table 1 next to the measured values. Figure 3 plots dispersion and absorption across the oxygen band at 800 mbar, illustrating the size of the interference effect.

Figure 4 compares the interference coefficients with two other sets. Liebe's³ were obtained using the model of Ref. 14, which relates the off-diagonal elements of M'' to the diagonal elements, and in which Liebe treated γ_0 as a free parameter, adjusting it to fit his measurements. Smith¹⁹ derived interference coefficients from a relaxation matrix that was computed by Lam¹² theoretically.

Table 2. Line-broadening coefficients and derived interference coefficients in air at 300 K. Linewidths are from Ref. 3, except that 1- is from Ref. 25 and the nonresonant coefficient is from Ref. 14.

N	Half-width (GHz/bar)		Interference (1/bar)	
	-	+	-	+
1	1.63	1.646	-0.0244	0.2772
3	1.468	1.449	-0.4068	0.6270
5	1.382	1.360	-0.6183	0.6766
7	1.319	1.297	-0.4119	0.3290
9	1.266	1.248	0.0317	-0.1591
11	1.221	1.207	0.1145	-0.2068
13	1.181	1.171	0.3398	-0.4158
15	1.144	1.139	0.3922	-0.4482
17	1.110	1.108	0.4011	-0.4442
19	1.079	1.078	0.4339	-0.4687
21	1.05	1.05	0.4783	-0.5074
23	1.02	1.02	0.5157	-0.5403
25	1.00	1.00	0.5400	-0.5610
27	0.97	0.97	0.5719	-0.5896
29	0.94	0.94	0.6046	-0.6194
31	0.92	0.92	0.6347	-0.6468
33	0.89	0.89	0.6627	-0.6718
nonresonant	0.48		0	

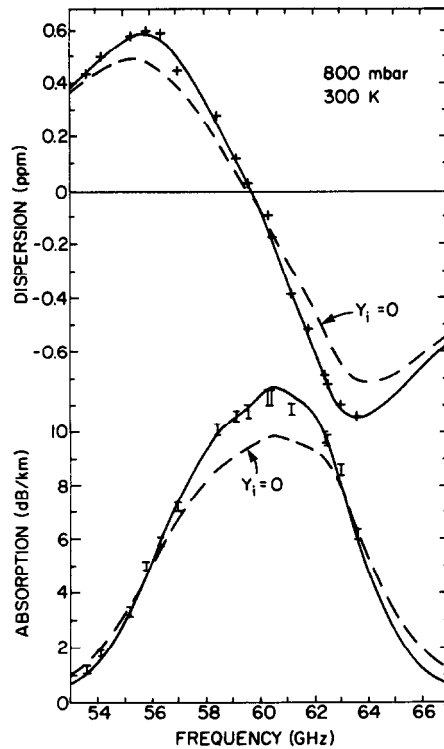


Fig. 3. Dispersion and absorption in dry air at 800 mbar (600 torr) pressure. —, Computed with interference coefficients from Table 2; ---, no interference. Measurements are from Ref. 1.

The interference coefficients are given to four decimal places in Table 2, only because precision will be lost when terms of opposite sign are summed. Errors in these values are correlated because of the linear transformation used to derive them from the measurements. The sensitivity of the spectrum to the interference coefficients can be judged by comparison with the other two sets of coefficients in Fig. 4. The coefficients from Table 2 fit the measurement in Table 1 slightly better (with 20 ppb r.m.s. residuals) than the coefficients of Liebe, which yield 28 ppb r.m.s. residuals. If

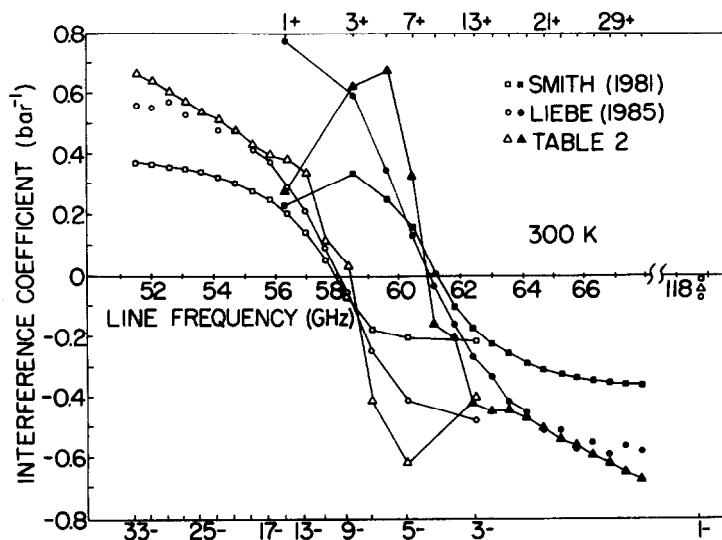


Fig. 4. Interference coefficients for lines in the oxygen microwave band.

one uses Smith's interference coefficients with Liebe's linewidths for air (perhaps not a proper thing to do), residuals of 56 ppb r.m.s. are obtained. However, Smith's interference coefficients may not be directly comparable with the other two sets, since Smith's are for pure oxygen, whereas Liebe's and those in Table 2 apply to oxygen lines broadened by dry air. The linewidths produced by air differ from those in oxygen at equal pressure by as much as 10% (at high values of N)² and it is conceivable that the off-diagonal elements of M'' differ by larger factors. Smith's paper shows a good fit of his calculations to measurements made by Liebe on pure oxygen, so it appears that the differences between the coefficients derived for air and Smith's coefficients are largely due to the different intermolecular potential for O_2-N_2 collisions vs O_2-O_2 collisions.

Some typical characteristics of the interference coefficients are illustrated by Fig. 4. The approximate antisymmetry of y_{N+} and y_{N-} is due to similarity of intra-branch submatrices in M'' , combined with the nearly even spacing of the line frequencies within each branch. The exception to this rule is the $1-$ line, whose resonant frequency is 118.75 GHz and which consequently has an interference parameter much smaller in magnitude than the $1+$ line. The interference parameters change sign near $N = 9$, which is the most populated level. This behavior seems to be related to the asymmetry in the relaxation matrix expressed by Eq. (7). Because interference parameters on the low side of the band are positive while those on the high side are negative, the interference effect lowers absorption on both sides and raises it in the middle. The effect is proportionally greatest on the far wings of the band, which are of interest for microwave transmission through the atmosphere; hence the importance of accurate values for these parameters.

4. ATMOSPHERIC TRANSMITTANCE

The inversion procedure described in the last section yields interference coefficients that fit the measurements from which they were derived. Logically, the next step should be to test these coefficients with other measurements. Of special interest are the band wings, which are difficult to measure in the laboratory but are important in transmission of millimeter waves between space and earth. In computing atmospheric absorption, however, it is necessary to consider the temperature dependence of the line parameters.

Most experimental treatments of line widths fit their pressure-temperature variation to a function P/T^x . Liebe³ uses $x = 0.8$. Although this treatment may be adequate for the linewidths, Eq. (7) implies that off-diagonal elements of the relaxation matrix cannot all have the same temperature dependence. Liebe's measurements of overlapped lines were done only at 300 K, but from the model relaxation matrix, he deduced a temperature dependence of the power-law form, with a different exponent for each of his interference coefficients. (Read et al³¹ found that this model reproduced the variation of absorption from 262 to 295 K.) The largest of Liebe's exponents³ apply to lines with $N \approx 9$. This result is connected with the smallness of the $9 \pm$ interference coefficients at 300 K, and with the variation with temperature of the value of N at which the sign change of the y s occurs. Aside from these idiosyncratic values, the exponents fall roughly into two groups: those at low N , which are approximately the same as the linewidth exponent, 0.8; and those at high N , which are higher by approximately unity.

Most of the atmospheric opacity on the oxygen band wings is contributed within a few kilometers of the surface. This circumstance should make it permissible to use a rough approximation to the variation of interference coefficients with temperature near 300 K. Accordingly, the following calculations assumed

$$y_{N\pm}(T) \sim \begin{cases} T^{-0.8}, & \text{for } N < 9; \\ T^{-1.8}, & \text{for } N \geq 9. \end{cases} \quad (20)$$

Plotted in Fig. 5 is zenith attenuation for the U.S. Standard Atmosphere, computed with coefficient from Table 2. Other parameters necessary to the computation are given in Ref. 3. The measurements are corrected for attenuation due to water vapor.† Attenuation at the two frequencies of 51.75 and 68.14 GHz provides an interesting test of the band shape, because the measured values

†Typically, this correction is done by measuring attenuation with the sun as a source, for many different values of precipitable water vapor. Attenuation is then extrapolated to zero precipitable water vapor by a regression line.

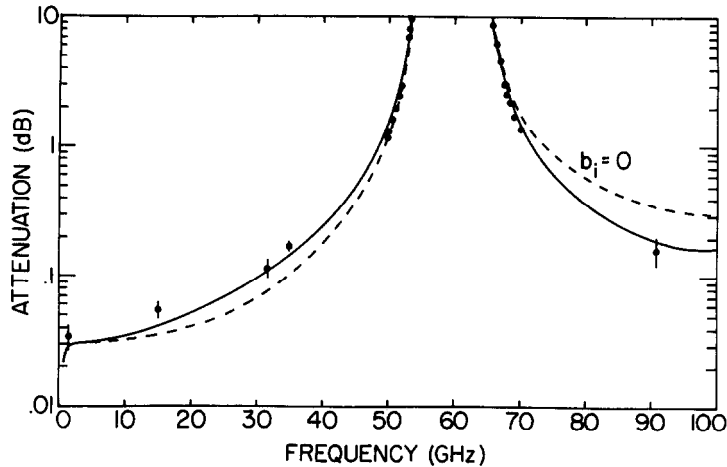


Fig. 5. Zenith attenuation due to oxygen in the 1962 U.S. Standard Atmosphere. Solid line uses interference coefficients from Table 2; dashed line uses interference coefficients computed without a bias term. Measurements are from Refs. 26–30.

are nearly equal: 2.43 ± 0.06 dB and 2.60 ± 0.05 dB, respectively.²⁶ The calculated values are 2.61 and 2.74 dB. The excess attenuation of <0.2 dB at both frequencies can be attributed to the very approximate temperature dependence assumed for the interference coefficients, and to the possibility that the temperature profile of the atmosphere in which the measurements were made was different from the U.S. Standard Atmosphere. However, if the interference coefficients are recalculated without the bias term given by Eq. (8), one obtains 2.32 and 3.19 dB respectively, an asymmetry in clear disagreement with the measurements. In general, the calculation including the bias in Fig. 5 conforms well to measurements out to the very far wings of the band. This result supports Gordon's¹⁸ theory for the band shape outside of the resonant region.

5. CONCLUSIONS AND RECOMMENDATIONS

The available dispersion measurements are of sufficient accuracy to derive useable interference coefficients for dry air at 300 K. One could also use absorption measurements if they were of comparable accuracy. However, the interference effect in absorption is strongest between line centers, so the absorption counterpart of Eq. (5) is somewhat more ill-conditioned.

Additional measurements to determine the variation with temperature of the interference coefficients would be desirable for the purpose of calculating radiative transfer in the atmosphere. It would also be of interest to investigate the influence of different perturber species.

Acknowledgements—The author thanks H. J. Liebe for providing data. This work was supported under an agreement with S. M. Systems and Research Corp.

REFERENCES

1. H. J. Liebe, G. G. Gimmetstad, and J. D. Hopponen, *IEEE Trans. Antennas Propag.* **AP-25**, 327 (1977).
2. H. J. Liebe and G. G. Gimmetstad, *Radio Sci.* **13**, 245 (1978).
3. H. J. Liebe, *Radio Sci.* **16**, 1183 (1981); **20**, 1069 (1985).
4. C. Cousin, R. Le Doucen, C. Boulet, A. Henry, and D. Robert, *JQSRT* **36**, 521 (1986).
5. M. O. Bulanin, A. B. Dokuchaev, M. V. Tonkov, and N. N. Filippov, *JQSRT* **31**, 521 (1984).
6. G. J. Rosasco, W. Lempert, W. S. Hurst, and A. Fein, *Chem. Phys. Lett.* **97**, 435 (1983).
7. M. Baranger, *Phys. Rev.* **111**, 494 (1958).
8. A. C. Kolb and H. Griem, *Phys. Rev.* **111**, 514 (1958).
9. U. Fano, *Phys. Rev.* **131**, 259 (1963).
10. U. Mingelgrin, Ph.D. Thesis, Harvard Univ., Cambridge, MA (1972).
11. U. Mingelgrin, "Classical Scattering Calculations for Diatomic Molecules," U.S. Dept. Commerce Rept. OT/TRER 32, U.S. Govt. Printing Office, Washington, D.C. (1972).

12. K. S. Lam, Ph.D. Thesis, Mass. Inst. Tech., Cambridge, MA (1976).
13. K. S. Lam, *JQSRT* **17**, 351 (1977).
14. P. W. Rosenkranz, *IEEE Trans. Antennas Propag.* **AP-23**, 498 (1975). The matrix w used in this reference is related to the relaxation matrix M'' by: $M''_{ij} = w_{ij}(2N_j + 1)^{1/2}(2N_i + 1)^{-1/2}$.
15. N. C. Grody, *J. Climate Appl. Met.* **22**, 609 (1983).
16. J. H. Van Vleck, *Phys. Rev.* **71**, 413 (1947).
17. U. Mingelgrin, *Mol. Phys.* **28**, 1591 (1974). The complex quantities W_i , λ_i used in this reference are related to the line parameters in Eqs. (1) and (2) by: $a_i = \text{Re}(W_i)$, $Y_i = \text{Im}(W_i)/a_i$, $v_i = -\text{Re}(\lambda_i)/2\pi$, $\gamma = -\text{Im}(\lambda_i)/2\pi$.
18. R. G. Gordon, *J. Chem. Phys.* **46**, 448 (1967).
19. E. W. Smith, *J. Chem. Phys.* **74**, 6658 (1981).
20. H. J. Liebe, *Rev. Sci. Instrum.* **46**, 817 (1975).
21. C. D. Rodgers, *Rev. Geophys. Space Phys.* **14**, 609 (1976).
22. A. Ben-Reuven, *Phys. Rev.* **145**, 7 (1966).
23. S. Twomey, *J. Ass. Comput. Mach.* **10**, 97 (1963); *J. Franklin Inst.* **279**, 95 (1965).
24. A. N. Tikhonov, *Dokl. Acad. SSSR* **151**, 501 (1963).
25. B. J. Setzer and H. M. Pickett, *J. Chem. Phys.* **67**, 340 (1977).
26. E. E. Reber, *J. Geophys. Res.* **77**, 3831 (1972).
27. D. C. Hogg, F. O. Guiraud, and E. R. Westwater, *Radio Sci.* **18**, 1295 (1983).
28. T. F. Howell and J. R. Shakeshaft, *J. Atmos. Terr. Phys.* **29**, 1559 (1967).
29. F. I. Shimabukuro and E. E. Epstein, *IEEE Trans. Antennas Propag.* **AP-18**, 485 (1970).
30. E. E. Altshuler, V. J. Falcone, and K. N. Wulfsberg, *IEEE Spectrum* **5**, 83 (1968).
31. W. G. Read, K. W. Hillig II, E. A. Cohen, and H. M. Pickett, *IEEE Trans. Antennas Propag.* (preprint 1987).